Dalton Transactions

Accepted Manuscript

This article can be cited before page numbers have been issued, to do this please use: T. Hirayama, A. Mukaimine, K. Nishigaki, H. Tsuboi, S. Hirosawa, K. Okuda, M. Ebihara and H. Nagasawa, *Dalton Trans.*, 2017, DOI: 10.1039/C7DT03194G.

ROYAL SOCIETY OF CHEMISTRY

rsc.li/dalton

View Article Online
DOI: 10.1039/C7DT03194G

Bismuth-rhodamine: a new red light-excitable photosensitizer

Tasuku Hirayama,[a] Akari Mukaimine,[a] Kenta Nishigaki,[a] Hitomi Tsuboi,[a] Shusaku Hirosawa,[a] Kensuke Okuda,[a,b] Masahiro Ebihara,[c] and Hideko Nagasawa[a]

[a]Laboratory of Pharmaceutical and Medicinal Chemistry, Gifu Pharmaceutical University, 1-25-4, Daigaku-nishi, Gifu, 501-1196, Japan.

[b] Current address: Laboratory of Bioorganic & Natural Products Chemistry, Kobe Pharmaceutical University, 4-19-1, Motoyamakita-machi, Higashinada-ku, Kobe, Hyogo, 658-8558, Japan.

[c] Department of Chemistry and Biomolecular Science, Faculty of Engineering, Gifu University, Yanagido, Gifu, 501-1193, Japan

Footnotes: Electronic Supplementary Information (ESI) available: Experimental details, pH titration of absorption and fluorescence spectra, fluorescence imaging data for EC_{50} measurements, NMR and mass data of the newly synthesized compounds. CCDC 1530802. For ESI and cyrystallographic data in CIF or other electronic format see DOI:xxxx.

Abstract

Bismuth-rhodamine (BiR) was developed as a new photosensitizer scaffold, and its photophysical properties were evaluated. BiR showed significant red-shifted absorption and emission compared with other xanthene-based photosensitizers together with an efficient quantum yield for generation of $^1O_2$. BiR showed easy cell-permeability as well as photo-triggered generation of $^1O_2$ in cells.

Bismuth (^{209}Bi) is the heaviest stable typical element. Unlike the other sixth row elements such as thallium, lead, and polonium, bismuth is known as a minimally toxic heavy element.[1] This factor enables the clinical use of bismuth compounds for antiflatulent such as bismuth subgallate (known as Dermatol® and Devrom®) and bismuth subsalicilate[2–9] for use in the treatment of gastrointestinal disorders. Organobismuth compounds have recently attracted attention as unique structural building blocks,[10] chemical reagents,[11–15] and phosphorescent materials.[16] Bismuth has the combination of low toxicity together with the characteristics of being a heavy atom. In this study, both these factors are explored with a view for the development of a new pharmaceutical organobismuth compound.

Both fluoresceins and rhodamines are categorized as xanthene fluorophores and have found wide application in various types of fluorescent probes.[17–19] Recently, several groups have reported that photophysical characteristics including excitation/emission wavelength could be tuned to the long wavelength region by a replacement of the oxygen atom within the xanthene core to the third row typical elements such as Si[20,21] and P.[22,23] Si-rhodamines show significantly red-shifted (~80 nm) absorption and emission compared to conventional rhodamines such as rhodamine B and have been widely utilized as red-emissive fluorophores.[24–27] Very recently, P-fluorescein[22] and

View Article Online
DOI: 10.1039/C7DT03194G

Si-rhodamines[23] have successively emerged as deep-red and near-infrared emissive fluorophores. Incorporation of the fourth or lower row chalcogen elements such as Se and Te into the xanthene ring by a replacement of the oxygen atom results in a relatively small red-shift (30–40 nm) of the excitation/emission together with efficient generation of an excited triplet state and subsequent singlet oxygen ($^1O_2$). This effect is a direct result of the elements with heavy atoms.[28–30] Chromophores that can generate $^1O_2$ upon irradiation of appropriate light have been utilized as photosensitizer of photodynamic therapy (PDT) of cancers.[31,32] An ideal photosensitizer should have a high absorption peak between 600 and 800 nm because the red to deep red absorption enable efficient tissue penetration of excitation light.[33] Additionally, no dark toxicity, water solubility, and high quantum yield for $^1O_2$ generation are also required for photosensitizes of PDT.[33] Conventional clinically used photosensitizers are composed of conjugated tetrapyrrole scaffolds such as porphyrin and chlorine but their synthetic difficulty, complexed structure, and large molecular sizes often hamper chemical modifications to improve their low water solubility, cellular uptake, and cancer selectivity.[31,33] Although photosensitizers consisting of fluoresceins and rhodamines chromophores could potentially be a good candidate as PDT agents due to the compatibility with chemical modifications and relatively high water solubility compared to the tetrapyrroles, the majority of them show absorption at less than 610 nm, which needs further effort to achieve efficient excitation under the tissue.[28–30,34] It has been reported by Oshita *et al*. that a 2,2'-bithiophene derivative bridged with phenylbismuth at 3 and 3'-position exhibited red-shifted absorption and emission compared to the corresponding carbon-bridged 2,2'-bithiophene, and the red-shift effect was compatible to its silicon-bridged counterpart.[16] These results prompted the investigation performed in this work, namely, to develop a bismuth-rhodamine (BiR) because dual effects of Bi-incorporation on excitation/emission wavelength and photosensitizing properties were expected. This investigation describes the preparation, structure, photophysical properties, and biological applications of BiR as a new scaffold for red light-excitable photosensitizers.

BiR was synthesized from bis(4-dimethylamino-2-bromophenyl)-2-tolyl-methane **1** *via* lithiation with *sec*-BuLi followed by treatment with $PhBiCl_2$ and oxidation with *p*-chloranil (Scheme 1). BiR was obtained in 4% yield from **1** as hexafluorophosphate salt after purification by recrystallization. The structure of BiR was characterized by ^{1}H-NMR, ^{13}C-NMR, and mass spectrometry, elemental analysis, and single crystal X-ray diffraction analysis.

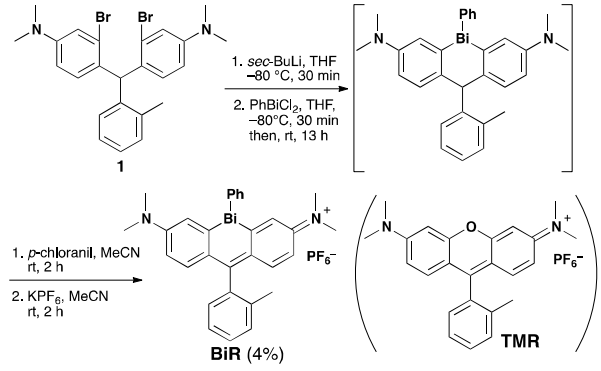

View Article Online
DOI: 10.1039/C7DT03194G

Scheme 1. Structures of BiR and TMR and synthetic procedure of BiR

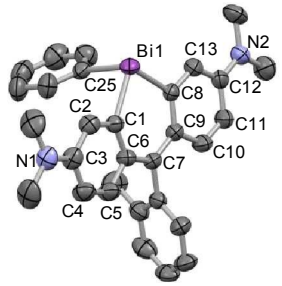

Fig. 1 ORTEP image of the structure of BiR (atomic displacement parameters: 50% probability, only selected atoms are labeled; hydrogen atoms, solvent (acetonitrile), and counter anion (PF_6^-) molecules are omitted for clarity. Gray: carbon. Blue: nitrogen. Purple: bismuth. Selected bond lengths (Å): Bi1–C1 = 2.226(5), Bi1–C8 = 2.236(5), Bi1–C25 = 2.283(7), C1–C2 = 1.389(6), C1–C6 = 1.426(7), C2–C3 = 1.412(6), C3–C4 = 1.407(8), C3–N1 = 1.349(6), C4–C5 = 1.361(7), C5–C6 = 1.405(7), C6–C7 = 1.432(6), C7–C9 = 1.418(6), C7–C18 = 1.508(7), C8–C9 = 1.428(7), C8–C13 = 1.361(6), C9–C10 = 1.449(7), C10–C11 = 1.331(7), C11–C12 = 1.411(8), C12–C13 = 1.421(7), C12–N2 = 1.335(6). Selected angles (°) C1–Bi1–C8 = 89.8(2), C1–Bi1–C25 = 92.4(2), C8–Bi1–C25 = 89.6(2), Bi1–C1–C2 = 116.1(4), Bi1–C1–C6 = 123.6(4), C2–C1–C6 = 120.2(5), C1–C2–C3 = 122.7(5), C2–C3–C4 = 116.4(5), C2–C3–N1 = 122.3(5), C4–C3–N1 = 121.2(5), C3–C4–C5 = 120.8(6), C4–C5–C6 = 124.1(6), C1–C6–C5 = 115.6(5), C1–C6–C7 = 126.2(5), C5–C6–C7 = 118.1(5), C6–C7–C9 = 129.3(5), C6–C7–C18 = 115.1(5), Bi1–C8–C9 =122.3(4), Bi1–C8–C13 = 115.0(4), C9–C8–C13 = 122.2(5), C7–C9–C8 = 127.3(5), C7–C9–C10 = 119.0(5), C8–C9–C10 = 113.7(5).

The structure of BiR obtained is shown in Fig. 1. The bismuth atom is fused into the xanthene plane by bridging the two phenyl rings with a bond angle of 89.8° (C1–Bi1–C8). Although two diastereomers may arise from the orientations of the pendant phenyl group on Bi and the methyl substituent of the *o*-tolyl group, BiR was isolated as a single isomer with the phenyl and methyl groups on the same side of the Bi-xanthene plane. The pendant phenyl ring bound to Bi1 is oriented perpendicularly to the Bi-xanthene ring (C1–Bi1–C25: 92.4°, C8–Bi1–C25: 89.6°). This right angle trigonal pyramidal geometry is a characteristic for organobismuth(III) compounds because the 6p orbital of the Bi atom participates in the C–Bi bonds without hybridization with the 6s orbital.[11,15,35,36] The Bi-fused six-membered ring Bi1–C1–C6–C7–C9–C8 has an extruded hexagonal planer geometry. Endocyclic bond angles at C1, C6, C7, C8, and C9 are much larger than 120° because of the extremely long Bi–C bonds (Bi1–C1 = 2.226, Bi1–C8 = 2.236 Å) and the small bond angle around the Bi atom (C1–Bi1–C8: 89.8°). The similar bond lengths of C3–N1 (1.349 Å) and C12–N2 (1.335 Å) are shorter than the typical single bond length as well as good planarity of the Bi-xanthene including methyl groups on N1 and N2 atoms suggest sp^2 property of N1 and N2 atoms, efficient de-localization of positive charge, and π-conjugation ranging from N1 to N2.

View Article Online
DOI: 10.1039/C7DT03194G

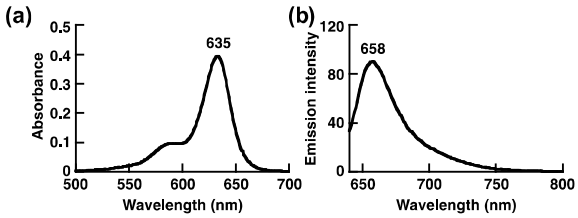

Fig.2 (a) Absorption spectrum of 5 μM BiR in 50 mM HEPES buffer (pH 7.4, 0.5% DMSO as a co-solvent) (b) Fluorescence spectrum of 2 μM BiR in 50 mM HEPES buffer (pH 7.4, 0.2% DMSO as a co-solvent). Excitation was provided at 630 nm.

Table 1. Photophysical properties of BiR and comparison with other xanthene-based fluorophores and photosensitizers

	heteroatom	λ_{abs} (nm)	ε (M^{-1} cm^{-1})	λ_{em} (nm)	Φ_{fl}	$\Phi(^1O_2)$
BiR	Bi	635	7.76×10^4	658	0.039	0.66
TMR	O	549	5.24×10^4	569	0.35	n.d.[g]
SiR650[a]	Si	646	11.0×10^4	660	0.31	n.d.[g]
NR_{666}[b]	P	666	16.5×10^4	685	0.38	n.d.[g]
MB[c]	N	660	5.08×10^4	n.d.[g]	n.d.[g]	0.52[f]
TMR-Se[d]	Se	581	4.4×10^4	n.d.[g]	0.009	0.87
TMR-Te[e]	Te	597	8.1×10^4	n.d.[g]	n.d.[g]	0.43

[a] Ref 25. [b]Ref 23 [c]MB = methylene blue. [d]Ref 29 (in methanol) [e]Ref 37 (in methanol). [f]Ref 38 (in acetonitrile). [g]Not determined.

The photophysical properties of BiR were evaluated in aqueous buffer (50 mM HEPES, pH 7.4, 0.2% or 0.5% DMSO as a co-solvent). BiR exhibited maximum absorption at 635 nm (ε = 77,600 M^{-1} cm^{-1}) and maximum emission at 658 nm (Figure 2), and these values are 86 nm and 91 nm red-shifted compared to tetramethylrosamine (TMR, Scheme 1) that has an oxygen-bridged xanthene scaffold (Table 1). Similar red-shifts have been observed in Si-rhodamine (SiR, λ_{abs} = 646 nm)[25] and P-rhodamine (NR_{666}, λ_{abs} = 666 nm)[23]. Such a large red-shift was not observed in the case for the heavy chalcogen atom-substituted rhodamines such as Se-rhodamine (TMR-Se, λ_{abs} = 581 nm)[29] and Te-rhodamine (TMR-Te, λ_{abs} = 597 nm).[28] The fluorescence quantum yield (Φ_{FL}) of BiR was determined to be 0.039, which is much lower than both SiR and NR_{666}. Both absorption and fluorescence are found to be insensitive to pH change (Fig. S1).

In order to fully understand the red-shifted photoproperties of BiR, electrochemical analysis and density functional theory (DFT) calculations were performed. Cyclic voltammograms of BiR and TMR are shown in Fig. 3a. Consideration of Fig. 3a indicates that BiR shows reversible peaks, thereby giving oxidation and reduction

View Article Online
DOI: 10.1039/C7DT03194G

potentials of 0.64 V and −0.99 V, respectively, while TMR provided potentials at 0.80 V and −1.20 V. The oxidation potential for BiR is 0.16 V lower than that for TMR. The reduction potential for BiR is 0.21 V higher than that for TMR, which suggests a smaller HOMO-LUMO gap of BiR than that of TMR. DFT calculations gave distinctly higher HOMO energy level for BiR than for TMR, while LUMO levels are not significantly different between these two compounds (Fg. 3b). No obvious participation of the Bi atom into HOMO nor LUMO were observed.

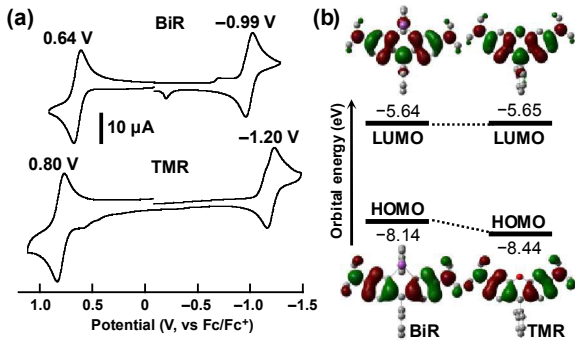

Fig. 3 (a) Cyclic voltammograms of BiR and TMR in acetonitrile (0.1 M tetrabutylammonium perchlorate as an electrolyte). The data were acquired with a glassy carbon electrode. The sample concentrations were 1 mM. The scan speed was 0.2 V s^{-1}. (b) Energy diagrams and HOMO/LUMOs for BiR and TMR calculated by using B3LYP/LANL2DZ set.

Because bismuth is the heaviest stable element, the heavy atom effect of Bi was expected to induce photo-generation of singlet oxygen ($^1O_2$) with BiR. The photo-generation of $^1O_2$ was evaluated by absorption spectroscopic analysis with a colorimetric $^1O_2$ scavenger, 1,3-diphenylisobenzofuran (DPBF, λ_{abs} = 410 nm) and methylene blue (MB) as a standard photosensitizer ($\Phi(^1O_2)$ = 0.52 in acetonitrile)[38,39]. Fig. 4 depicts the spectral changes of DPBF in the presence of BiR (Fig. 4a) and MB (Fig. 4b) upon irradiation with red LED light (λ_{ex} = 625 nm, 1.2 mW cm^{-2}). Upon irradiation by red light, a significant decrease in absorption of DPBF at 410 nm was observed for BiR over a period of 500 s ($k_{obs} = -1.87\times10^4$ s^{-1}), while a relatively slow decrease was seen for MB ($k_{obs} = -1.47\times10^4$ s^{-1}) (Fig. 4d). No apparent change was found in the absence of irradiation (Fig. 4c,d). The $\Phi(^1O_2)$ of BiR was calculated to be 0.66 on the basis of initial consumption rates of DPBF. Integrated with the high molar absorption (ε_{635} = 77,600 M^{-1} cm^{-1}), BiR is found to be two times more efficient than MB (ε_{660} = 50,800 M^{-1} cm^{-1}). Under the same irradiation condition, the photo-induced degradation of BiR was 15% over 1 h, and MB showed 10% degradation (Figure S2), indicating that the photostability of BiR is comparable to that of MB. Taking the above observations into account suggests that BiR could act as a new red light-excitable photosensitizer.

View Article Online
DOI: 10.1039/C7DT03194G

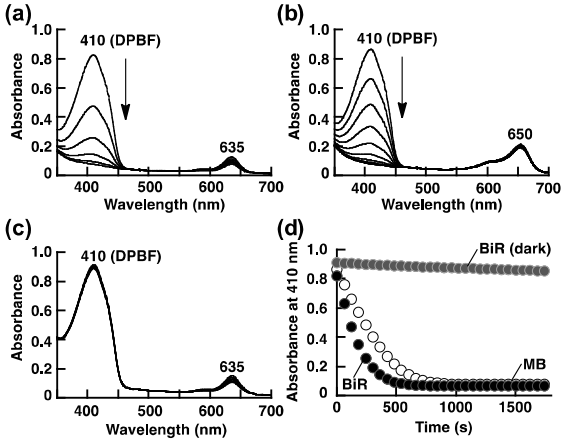

Fig. 4 Absorption spectral changes of DPBF upon irradiation of red light (625 nm, 1.2 mW cm^{-2}) in the presence of BiR (a) and MB (b). The concentration of the photosensitizers and DPBF were set to show absorption of 0.2 at 625 nm and 0.8 at 410 nm, respectively. (c) Absorption spectral change of DPBF without irradiation in the presence of BiR. (d) Plot of absorption at 410 nm measured in (a), (b), and (c) against time. The data was collected every 60 s.

The photosensitizing ability of BiR under subcellular conditions was also evaluated. Two cancer cell lines were selected, namely, hepatocellular carcinoma cells (HepG2) and human lung adenocarcinoma cells (A549) as well as non-cancerous cell lines, human embryonic kidney cells (HEK293) and normal human diploid cells (TIG-3). The cell viability after irradiation with red light (608–648 nm, 9.0 J cm^{-2}) was assayed by measuring the population of cells stained with propidium iodide (PI). The typical images used for the viability analysis of HepG2 cells are shown in Fig. 5a. Fluorescence microscopic studies revealed that BiR can easily permeate cell membranes and brightly stain the perinuclear region that was determined as endoplasmic reticulum (Fig. S3). No obvious cell death occurred without irradiation in the presence of BiR (Fig. 5a, middle column), indicating that the negligible acute toxicity of BiR (Figure S8). Red-light irradiation caused a significant increase in the population of dead cells (Fig. 5a, right column), while irradiation in the absence of BiR resulted in no cell death (Fig. 5a, left column). The dead cells increased in a dose-dependent manner with BiR under the irradiated conditions (Fig. 5b, Fig. S8), and the EC_{50} value, which is defined as the concentrations for 50% cell death under irradiation, was determined to be 375 nM for HepG2 cells (Fig 5c). EC_{50} values for the other cells were also determined as follows: A549 (11 nM), HEK293 (40 nM), and TIG-3 (20 nM). BiR showed moderate toxicity for the cells used in this study (IC_{50} = 0.53 μM (HepG2), 0.62 μM (A549), 2.26 μM (HEK293), and 0.96 μM (TIG-3)) when the cells were treated with BiR for 24 h in dark conditions (Figure 5c and S9). In this study, tumor-selectivity of BiR itself could not be observed, but its efficient ability to produce $^1O_2$ even under subcellular conditions indicates that it is a promising candidate to be used as an alternative to present photosensitizers.

In summary, we successfully synthesized a bismuth-containing analogue of rhodamine, BiR. Incorporation of bismuth into a rhodamine scaffold provided the chromophore with dual functionalities, namely, red-shift and

View Article Online
DOI: 10.1039/C7DT03194G

photo-generation of $^1O_2$. This result shows that BiR can act as a new red light-excitable photosensitizer. The absorption and emission of BiR was red-shifted compared to its corresponding tetramethylrhodamine and xanthene-based photosensitizers with heavy chalcogen atoms (Se and Te). Furthermore, it was shown that BiR can generate $^1O_2$ upon red-light irradiation more efficiently than a known conventional red-light-excitable photosensitizer, methylene blue (MB). This is due to the large molar absorption as well as high quantum yield $\Phi(^1O_2)$ of BiR. Photosensitization of BiR was demonstrated in live cells and that the EC_{50} for the cells were nano-molar in range. Red light has a great penetration properties and is therefore effective for the treatment of deep targets in the body by photodynamic therapy (PDT). Preliminary application of BiR to photodynamic treatment of a mouse xenograft model was performed, and unfortunately unexpected results were obtained. Although fluorescence signal of BiR was observed stably in the xenograft tumor through the whole mouse in vivo imaging, degradation of BiR unexpectedly proceeded upon irradiation (data not shown). Since BiR is stable against either of irradiation (Figure S2) or subcellular condition, we speculate that decomposition of BiR would be accelerated especially upon photo-irradiation in the presence of biological chemical species and that excited state of BiR would be susceptible to intravital environments. Therefore, BiR could be an attractive pharmaceutical scaffold for a new photosensitizer for PDT because of its red-light excitation and $^1O_2$-generation properties. Further studies on structural modifications of this compound with a view to targeting cancer as well as an improvement in its *in vivo* photo-stability are currently in progress and will be the subject of future published research.

We thank Prof. Shinae Kondoh and Dr. Takahiro Kuchimaru (Tokyo Institute of Technology) for their help for preliminary mice xenograft experiments. We also thank Prof. Yukio Yamamoto, Dr. Masayasu Taki, and Ms. Naoko Sakai (Kyoto University) for their help for X-ray diffraction analysis and Ms. Emi Inaba for her technical assistance. This work was financially supported by JSPS KAKENHI (no. 15K14981 for T.H.).

View Article Online
DOI: 10.1039/C7DT03194G

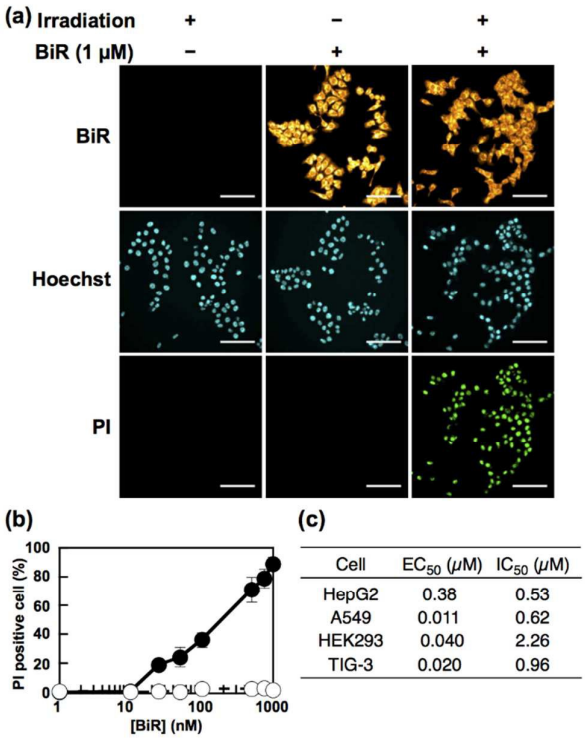

Fig.5 (a) Representative fluorescence images of HepG2 cells stained with BiR followed by PI/Hoechst. Left column: Images of the irradiated cells without BiR staining. Middle column: Images of the non-irradiated cells stained with BiR. Right column: Images of the irradiated cells stained with BiR. All the cells were treated with a mixture of PI and Hoechst 33342 after irradiation. The irradiation was done with Scale bars indicate 100 μm. (b) Plot of the population of PI-positive cells against BiR concentration with irradiation (filled circles) and without irradiation (open circles). (c) Table of the calculated EC_{50} and IC_{50} of various cells. EC_{50} was defined as the concentrations at which 50% cell death were observed under irradiation condition. IC_{50} was defined as the concentration at which 50% cell death were observed after treatment for 24 h.

References

1 Y. Hong, Y.-T. Lai, G. C.-F. Chan and H. Sun, *Proc. Natl. Acad. Sci. U. S. A.*, 2015, **112**, 3211–3216.

2 L. M. Mai, C. Y. Lin, C. Y. Chen and Y. C. Tsai, *Biomaterials*, 2003, **24**, 3005–3012.

3 V. A. Tramontina, M. A. N. Machado, G. da R. Nogueira Filho, S. H. Kim, M. R. Vizzioli and S. de Toledo, *Braz. Dent. J.*, 2002, **13**, 11–16.

4 R. Burns, D. W. Thomas and V. J. Barron, *Br. Med. J.*, 1974, **1**, 220–223.

5 K. D. Fine and E. L. Lee, *Gastroenterology*, 1998, **114**, 29–36.

6 H. L. DuPont, *Nat. Clin. Pract. Gastroenterol. Hepatol.*, 2005, **2**, 191–198.

View Article Online
DOI: 10.1039/C7DT03194G

7 H. Li and H. Sun, *Curr. Opin. Chem. Biol.*, 2012, **16**, 74–83.

8 D. M. Keogan and D. M. Griffith, *Molecules*, 2014, **19**, 15258–15297.

9 G. G. Briand and N. Burford, *Chem. Rev.*, 1999, **99**, 2601–2657.

10 S. L. Benjamin and G. Reid, *Coord. Chem. Rev.*, 2015, **297**–**298**, 168–180.

11 L. D. Freedman and G. O. Doak, *Chem. Rev.*, 1982, **82**, 15–57.

12 T. Ooi, R. Goto and K. Maruoka, *J. Am. Chem. Soc.*, 2003, **125**, 10494–10495.

13 K. Ikegai, K. Fukumoto and T. Mukaiyama, *Chem. Lett.*, 2006, **35**, 612–613.

14 P. Petiot and A. Gagnon, *European J. Org. Chem.*, 2013, 5282–5289.

15 H. Suzuki, T. Ikegami and Y. Matano, *Synthesis (Stuttg).*, 1997, **1997**, 249–267.

16 J. Ohshita, S. Matsui, R. Yamamoto, T. Mizumo, Y. Ooyama, Y. Harima, T. Murafuji, K. Tao, Y. Kuramochi, T. Kaikoh and H. Higashimura, *Organometallics*, 2010, **29**, 3239–3241.

17 K. P. Carter, A. M. Young and A. E. Palmer, *Chem. Rev.*, 2014, **114**, 4564–4601.

18 J. Chan, S. C. Dodani and C. J. Chang, *Nat. Chem.*, 2012, **4**, 973–984.

19 L. D. Lavis and R. T. Raines, *ACS Chem. Biol.*, 2014, **9**, 855–866.

20 M. Fu, Y. Xiao, X. Qian, D. Zhao and Y. Xu, *Chem. Commun.*, 2008, 1780–1782.

21 Y. Koide, Y. Urano, K. Hanaoka, T. Terai and T. Nagano, *ACS Chem. Biol.*, 2011, **6**, 600–608.

22 A. Fukazawa, S. Suda, M. Taki, E. Yamaguchi, M. Grzybowski, Y. Sato, T. Higashiyama and S. Yamaguchi, *Chem. Commun.*, 2016, **52**, 1120–1123.

23 X. Zhou, R. Lai, J. R. Beck, H. Li and C. I. Stains, *Chem. Commun.*, 2016, **52**, 12290–12293.

24 S. Kim, T. Tachikawa, M. Fujitsuka and T. Majima, *J. Am. Chem. Soc.*, 2014, **136**, 11707–11715.

25 Y. Koide, Y. Urano, K. Hanaoka, W. Piao, M. Kusakabe, N. Saito, T. Terai, T. Okabe and T. Nagano, *J. Am. Chem. Soc.*, 2012, **133**, 5029–5031.

26 G. Lukinavičius, K. Umezawa, N. Olivier, A. Honigmann, G. Yang, T. Plass, V. Mueller, L. Reymond, I. R. Corrêa, Z.-G. Luo, C. Schultz, E. a Lemke, P. Heppenstall, C. Eggeling, S. Manley and K. Johnsson, *Nat. Chem.*, 2013, **5**, 132–139.

View Article Online
DOI: 10.1039/C7DT03194G

27 T. Myochin, K. Hanaoka, S. Iwaki, T. Ueno, T. Komatsu, T. Terai, T. Nagano and Y. Urano, *J. Am. Chem. Soc.*, 2015, **137**, 4759–4765.

28 M. W. Kryman, G. A. Schamerhorn, J. E. Hill, B. D. Calitree, K. S. Davies, M. K. Linder, T. Y. Ohulchanskyy and M. R. Detty, *Organometallics*, 2014, **33**, 2628–2640.

29 T. Y. Ohulchanskyy, D. J. Donnelly, M. R. Detty and P. N. Prasad, *J. Phys. Chem. B*, 2004, **108**, 8668–8672.

30 Y. Ichikawa, M. Kamiya, F. Obata, M. Miura, T. Terai, T. Komatsu, T. Ueno, K. Hanaoka, T. Nagano and Y. Urano, *Angew. Chem. Int. Ed. Engl.*, 2014, **53**, 6772–6775.

31 R. R. Allison and C. H. Sibata, *Photodiagnosis Photodyn. Ther.*, 2010, **7**, 61–75.

32 P. Agostinis, K. Berg, K. a Cengel, T. H. Foster, A. W. Girotti, S. O. Gollnick, S. M. Hahn, M. R. Hamblin, A. Juzeniene, D. Kessel, M. Korbelik, J. Moan, P. Mroz, D. Nowiz, J. Piette, B. C. Willson and J. Golab, *Am. Cancer Soc.*, 2011, **61**, 250–281.

33 M. R. Detty, S. L. Gibson and S. J. Wagner, *J. Med. Chem.*, 2004, **47**, 3897–3915.

34 J. E. Hill, M. K. Linder, K. S. Davies, G. A. Sawada, J. Morgan, T. Y. Ohulchanskyy and M. R. Detty, *J. Med. Chem.*, 2014, **57**, 8622–8634.

35 A. Soran, H. J. Breunig, V. Lippolis, M. Arca and C. Silvestru, *Dalton Trans.*, 2009, **2**, 77–84.

36 A. Schulz and A. Villinger, *Organometallics*, 2011, **30**, 284–289.

37 B. Calitree, D. J. Donnelly, J. J. Holt, M. K. Gannon, C. L. Nygren, D. K. Sukumaran, J. Autschbach and M. R. Detty, *Organometallics*, 2007, **26**, 6248–6257.

38 Y. Usui, H. Koike and Y. Kurimura, *Bull. Chem. Soc. Jpn.*, 1987, **60**, 3373–3378.

39 N. Adarsh, R. R. Avirah and D. Ramaiah, *Org. Lett.*, 2010, **12**, 5720–5723.

View Article Online
DOI: 10.1039/C7DT03194G

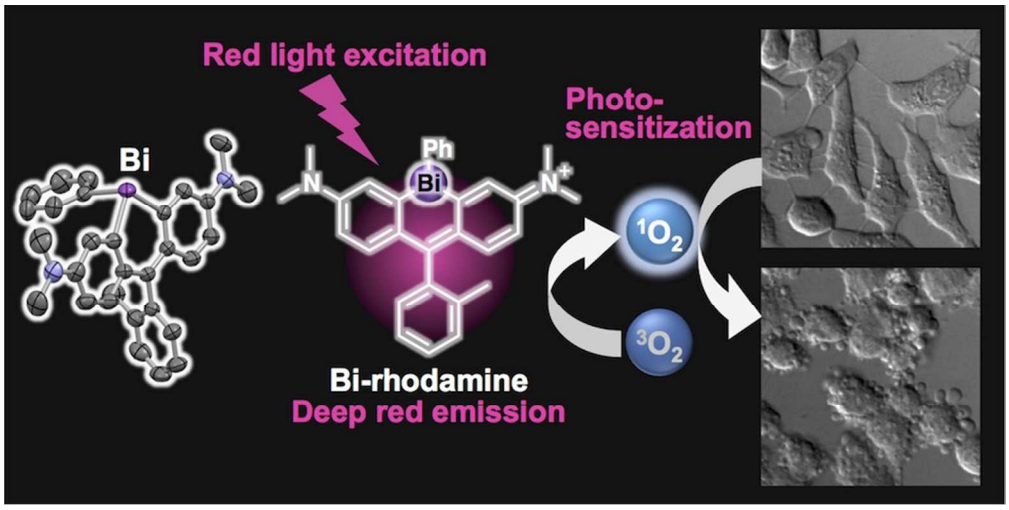

80x39mm (300 x 300 DPI)

View Article Online
DOI: 10.1039/C7DT03194G

A new red-light excitable photosensitizer, Bi-rhodamine, was developed.